

PROTECTION PROBLEM FOR THIN-WALLED COMPOSITE CONSTRUCTIONS OF AIRCRAFT FROM ACTION OF RADIATIONS AND PARTICLES FLUXES

Ostrik A.V.*, Bakulin V.N.** , Matveenko A.M.***

*Institute of Problems of Chemical Physics RAS, Chernogolovka, Russia

**Institute of Applied Mechanics RAS, Moscow, Russia

***Moscow Aviation Institute, Moscow, Russia

Keywords: radiation, heterogeneous sheetings, composites, shells

Abstract

The settlement and experimental method for verification of strength of thin-walled composite aircraft (AC) constructions to action of radiations and particles fluxes (RPF) having various physical nature is offered. The scientific and methodical technology realizing this method is considered.

Various versions of constructional methods of aircraft protection are investigated.

1 Introduction

The High-modular Composite Materials (HMCM) find the increasing application in carrier constructions for aircraft and cosmic techniques. HMCM have a set of properties reducing their resistance to different types of RPF actions in comparison with traditional constructional materials (metals and their alloys). In particular the lowered HMCM conductivity leads to strengthening of charge effects role at RPF action. Low radiation resistance of the HMCM components is the reason of untimely ageing and degradation of deformation and strength properties. In additives principal heterogeneity and anisotropy of composites complicate an assessment of parameters of RPF actions. For these reasons HMCM application demands additional measures for protection of aircraft constructions [1,2].

The set of external layers of the shielding coverings having highly specialized

appointment (antistatic, damping, radio absorbing, etc.) is used as RPF protection.

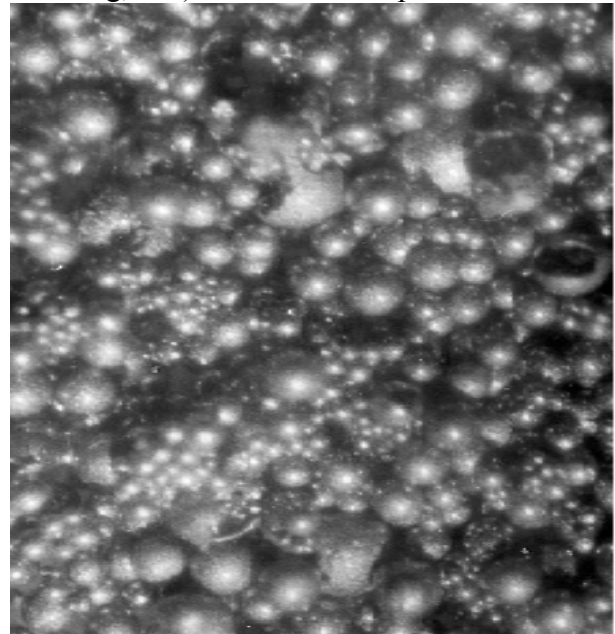


Fig. 1. Glass MS having a tungsten covering

But recently universal heterogeneous sheetings (HS) are created. These HS unite functions of several specialized coverings. In particular, HS made of epoxies or rubbers and fillers consisting of the hollow metalized microspheres (MS) possess the unique protective properties. These HS are the hollow-sphere plastics. Use of inorganic microspheres made of carbon or glass (fig. 1) is the most perspective. First hollow-sphere plastics weaken influencing RPF by means of the heavy metals raised dust on filler. Secondly bodies damp a being formed mechanical impulse owing to an irreversible MS collapse.

2 The settlement and experimental method

In the present work charging thermal and mechanical RPF actions directed on thin-walled composite aircraft constructions having heterogeneous sheetings are considered. The settlement and experimental method is offered [2]. Forecasting of parameters of RPF actions becomes a settlement way. Verification of constructions strength to heat and mechanical loadings having these settlement parameters is carried out by means of natural tests for elements of composite aircraft constructions.

The main components of the scientific and methodical technology realizing offered method and some examples for a case of influence of the ionizing radiation (IR) are considered further.

3 Calculation of parameters of RPF actions

3.1 The absorbed energy and currents

Characteristics of spatio-temporal distributions of the absorbed energy and electric currents are initial data for calculation of parameters of RPF actions. The Monte-Carlo method is used for numerical modeling of RPF propagation and absorption taking place in materials of aircraft constructions. The hybrid method [3] is offered. RPF transfer is modeled by a statistical method. Energy redistribution (by secondary electronic radiation) being realized between the HS components is considered analytically.

The knowledge of parts of the energy absorbed in components of a material is required for calculation of parameters of thermomechanical IR action [1] realized on GS. Spectrum of IR changes in process of radiation propagation into barriers. This change is the reason of dependence of absorbed energy parts from mass coordinate.

We assume that parameters of radiation flux do not change within a cell (length of photons run took place on HS significantly more than sizes of disperse inclusions) and application of a method of "inserts" [1] is admissible. The essence of a method of "inserts" consists that the IR parameters are defined for a homogeneous

material having average characteristics (for example, by means of a statistical method of density of collisions [4]). Then the elementary GS cell is took place at different distances from an irradiated surface. Calculation of energy redistribution by electrons is carried out in this cell. When performing the conditions stated above the number of electrons $n_i(E, E_{ph})dE$ born in unit of volume with energy from E to $E + dE$ at radiation flux is equal to one photon (with energy E_{ph}) per unit area, doesn't depend on spatial coordinates for each i - layer of a spherical cell. In addition electrons distribution on the directions of a departure is supposed isotropic [5]. Then parts of the energy absorbed in cell layers ε_j are defined by a formula [3]

$$\varepsilon_j = \frac{\int_{E_{phmin}}^{E_{phmax}} dE_{ph} F(E_{ph}) \sum_{i=1}^N \int_0^{E_{max}} n_i(E, E_{ph}) V_i P_{ji}(E) EdE}{\sum_{j=1}^N \int_{E_{phmin}}^{E_{phmax}} dE_{ph} F(E_{ph}) \sum_{i=1}^N \int_0^{E_{max}} n_i(E, E_{ph}) V_i P_{ji}(E) EdE}, \quad (1)$$

where V_i – the volume of i -layer; $F(E_{ph})$ – normalized partial IR spectrum located in points of an insert of a cell in an average material; $P_{ji}(E)$ – energy part (pays off in the assumption of equal density of the birth of electrons within a layer) given by electrons in j -layer at their birth in i -layer (it is obviously that $\sum_{j=1}^N P_{ji}(E) \equiv 1$). We note that to the requirement $\sum_{j=1}^N \varepsilon_j = 1$ is carried out for a formula (1). But value entering a denominator of a formula (1) satisfies only to an inequality (equality is reached at photon death as a result of interaction with cell components, however interactions can not be):

$$\sum_{j=1}^N \int_0^{E_{phmax}} dE_{ph} F(E_{ph}) \sum_{i=1}^N \int_0^{E_{max}} n_i(E, E_{ph}) V_i P_{ji}(E) EdE \leq E_{ph}.$$

Thus transposition properties of electrons in a cell are set by functions P_{ij} . These are functions depend on one value by one value (it is electron energy E) if accepted assumptions are valid.

We will consider calculation of functions $P_{ji}(E)$ and $n_i(E, E_{ph})$. Is admissible to accept that secondary electrons are absorbed in a layer

of their birth at rather small energy $E \leq E_{\min}$ (at calculations it was $E_{\min} \cong 10\kappa\epsilon B$) and then

$$P_{ii}(E) \equiv 1, P_{ji}(E) \equiv 0 \text{ if } E \leq E_{\min} \text{ and } j \neq i.$$

It is inadmissible to consider that the electron is absorbed in a point of the birth when electron energy is $E > E_{\min}$. Then we find for functions $P_{ji}(E)$:

$$P_{ji}(E) = \frac{4\pi}{V_i} \int_{R_{i,\min}}^{R_{i,\max}} r^2 dr \int_0^{\pi} \frac{1}{2} \sin(\varphi) p_{ji}(r, \varphi, E) d\varphi = \quad (2)$$

$$= \frac{2\pi}{V_i} \int_{R_{i,\min}}^{R_{i,\max}} r^2 dr \int_0^{\pi} \sin(\varphi) p_{ji}(r, \varphi, E) d\varphi,$$

where $p_{ji}(r, \varphi, E)$ – the parts of energy given by an to j -layer at its birth in i -layer; φ – corner between the direction of movement of an electron and the radial direction; r – distance from the cell center. Calculation of functions $p_{ji}(r, \varphi, E)$ is workable if cell geometry and loss of electron energy $dE/dm = -f(E)$ (m – mass distance passed by an electron) are known. Required functions $P_{ji}(E)$ are fined by means of numerical determination of multiple integral located in the right part (2) if functions $p_{ji}(r, \varphi, E)$ are known already. When we calculate functions $p_{ji}(r, \varphi, E)$ electron trajectory is replaced with the reflected trajectory if the electron comes to cell boundary. This procedure takes into account arrival of electrons from the next cells with parameters corresponding to a considered electron

Functions $n_j(E, E_{ph})$ of density of the electrons birth represent the sum of the particles which are forming at photo-absorption and Compton's scattering (absorption is absent at Rayleigh and this scattering influences only on photons transfer):

$$n_i(E, E_{ph}) = n_i^f(E, E_{ph}) + n_i^c(E, E_{ph}).$$

We will consider for simplicity of calculation of energy release that all photoelectrons are absorbed in a birth point except for electrons taking off from a cover K. Then these electrons can be distributed evenly on energy interval $(0, E_{\min})$. Electrons having total energy I_K (energy of an exit of an electron from a -cover K) are added also in this interval (such electrons isn't formed but their

introduction allows to consider common the energy absorbed in a point of interaction as a result of atom ionization). It is supposed that only one photoelectron is formed in each photoabsorption (Auger electrons are considered also as a particle absorbed in an interaction point). Then we receive:

$$n_i^f(E, E_{ph}) = \begin{cases} \frac{2E_{ph}}{E_{\min}^2} \rho_i \sigma_i^f(E_{ph}) \theta(E_{\min} - E), & E_{ph} \leq E_K, \\ \rho_i \sigma_i^f(E_{ph}) \left[\delta(E - (E_{ph} - I_K)) + \frac{2I_K}{E_{\min}^2} \theta(E_{\min} - E) \right], & E_{ph} > E_K, \end{cases} \quad (3)$$

where $\delta(E)$, $\theta(E)$ – delta- and theta- functions, respectively; ρ_i , $\sigma_i^f(E_{ph})$ – density and mass coefficient of photoabsorption of the material of i -layer. Function of density of the birth of Compton electrons is written out similarly:

$$n_i^c(E, E_{ph}) = \begin{cases} \frac{2E_{ph}}{E_{\min}^2} \rho_i \sigma_i^c(E_{ph}) \theta(E_{\min} - E), & E_{ph} \leq E_{\min}, \\ \frac{m_e c^2}{2} \rho_i \sigma_i^c(E_{ph}) \frac{1}{(E_{ph} - E)^2}, & E_{ph} > E_{\min}, \end{cases} \quad (4)$$

where $m_e c^2$ – rest energy of electron.

We note that need arises to distribute evenly (for $E \leq E_{\min}$) spectrum of Compton's electrons forming at action of low energy photons. It is required as function $n_i^c(E, E_{ph})$ (4) (for $E_{ph} > E_{\min}$) is received from Compton's formula valued for interaction being realized between a photon and a free electron. It is quite admissible that we ignore binding energy of an electron and atom for $E_{ph} > E_{\min}$ and $E_{\min} \cong 10keV$. We will note also that isotropy of angular distribution of Compton's electrons is supposed in a formula (4). It was assumed earlier in (1). But it is known that this assumption isn't carried out for Compton's electrons. This fact is an essential defect of a method at calculation of secondary electrons currents of for forecasting of charging effects. But the direction of carrying out of energy appears less important for calculation of redistribution of energy between components of the heterogeneous environment. Here the fact of carrying out of energy from one component to another is basic. Besides angular distribution of secondary electrons is almost isotropic if photons energy is in x-ray range. Photons energy is small in comparison with rest energy of electrons for this range.

As an example we will consider results of calculations of functions $P_{ji}(E)$ (2) for hollow-sphere plastics consisting of epoxy-polyamide composition (EPC) and fillers made from the glass (carbon) microspheres covered with tungsten (nickel).

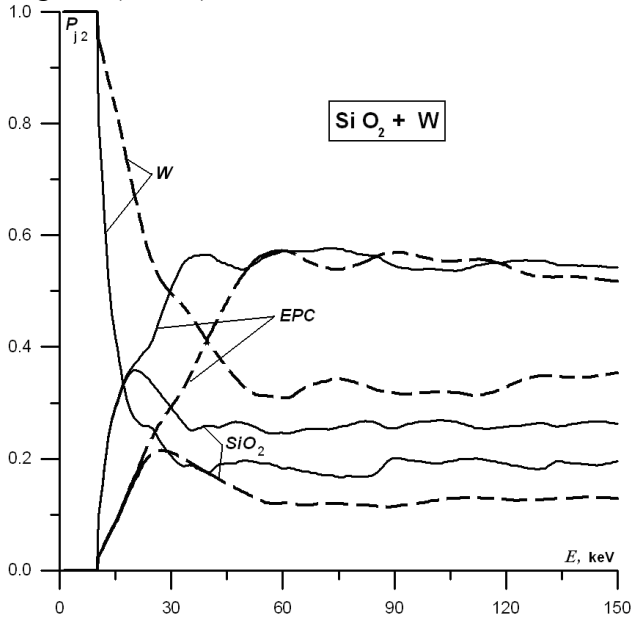


Fig. 2. Part of an energy output from tungsten in glass MS

Internal radius and thickness (without covering) are considered constant and equal $R_{MS} = 50\mu m$ and $h_{MS} = 2\mu m$ respectively.

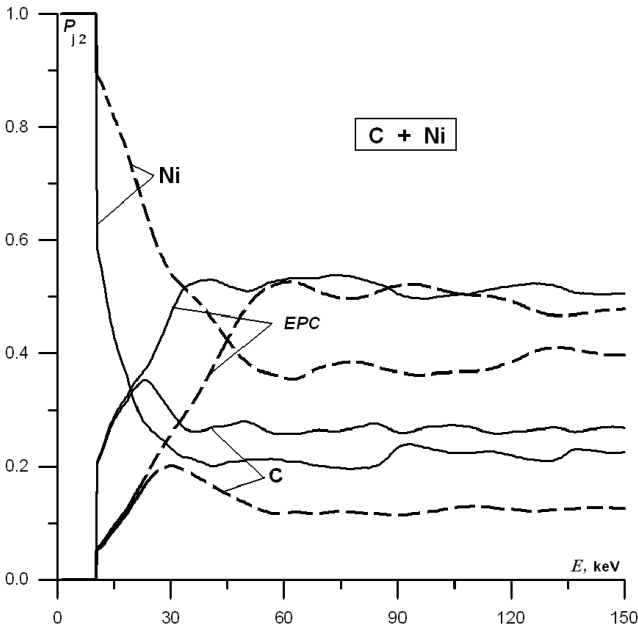


Fig. 3. Part of an energy output from nickel in carbon MS

Mass concentration of a filler is fixed also $m_f = 45\%$. Results of calculations of an energy output from tungsten ($i=2$) by means of electrons are presented in fig. 2 for various mass concentrations of tungsten containing in MS = 50% (continuous lines); 80% (dashed lines). It is visible that the part of the taken-out energy falls with growth of the mass tungsten concentration and decrease in electrons energy because the relation of electron run length to thickness of a tungsten layer decreases. Similar results ($R_{MS} = 50\mu m, h_{MS} = 2\mu m, m_f = 45\%$) for hollow-sphere plastics having the carbon MS covered with nickel ($i=2$) are presented in fig. 3.

As appears from the received results, parts of an energy output by means of electrons for considered microspheres are approximately equal at identical mass concentration of HS components and the MS sizes (carrying out appears a little more intensive in case of a tungsten dusting).

3.2 Mechanical RPF action

Parameters of mechanical RPF action are formed in the irradiated HS intensively absorbing radiations and particles. As a rule RPF absorption leads to temperature non-equilibrium of the HS components. Set of elementary cells of HS [1] having disperse high-porous filler (for example the multilayered microspheres covered with heavy metals) is offered for the accounting of HS heterogeneity (in particular for non-equilibrium generated by heterogeneity).

In case of the small specific absorbed energy Q and absence of phase transitions the formula [6] can be used for determination of coefficient of generation of thermal pressure Γ_{eff} (effective Gruneisen coefficient determining thermomechanical pressure $P = \Gamma_{eff} \rho Q$) taking into account elastic shift tension took place in HS binder

$$\Gamma_{eff} = \frac{\rho_f \rho_b}{\rho_0} \frac{\Gamma_f \varepsilon_f \bar{K}_b + \Gamma_b \varepsilon_b \bar{K}_f}{m_f \rho_b \bar{K}_b + m_b \rho_f \bar{K}_f}, \quad \bar{K}_{f,b} = K_{f,b} + \frac{4}{3} G_b,$$

where indexes 0, b, f designate HS as a whole, binder and filler respectively; $m, \varepsilon, \Gamma, \rho, K$ (having corresponding indexes) – mass

concentration, parts of the absorbed energy, Gruneisen coefficients, density and modules of volume compression of HS components; G_b - module of binder shift. We note that at $G_b = 0$ this relationship between the Gruneisen coefficient Γ_{eff} and material properties passes into known Anderkholm's relationship [7] received in hydrodynamic approach.

Plastic current regions of a binder can be formed near strongly absorbing grains of a filler if the specific absorbed energy and warming up of HS components increase [8, 9]. In this case not accounting of change of mechanical material characteristics is the reason of errors of calculation of mechanical radiation action took place on HS.

Regions of change of energy release parameters of (Q, ε_f) received on model [8] are presented in fig. 4. Various conditions of the binder are realized in these regions. They are elastic, mixed (binder near MS is in a plastic state; the periphery of a cell is in elastic), purely plastic and hydrodynamic conditions. Apparently from fig. 4 the region of plasticity takes place practically in all range of change of the specific energy Q (this energy absorbed in HS) representing practical interest.

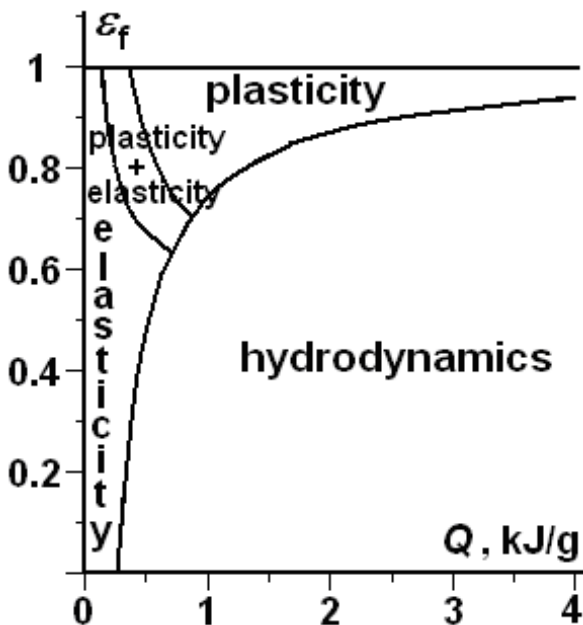


Fig. 4. Regions of a states of binder EDT-10. The filler is carbon MS covered with nickel

Destruction of a microspherical HS filler needs to be considered at rather big levels of IR energy release. We receive system of three

ordinary nonlinear differential equations for three unknown functions (specific internal energy of HS components E_f , E_b , and P pressure P) depending on specific energy Q , absorbed in shiting if we use condition of incompressibility of an elementary HS cell together with the first beginning of thermodynamics for filler and binder separately ($i=f, b$):

$$\left\{ \begin{aligned} \sum_{j=f,b} \frac{m_j}{\rho_j(P, E_j)^2} \left(\left(\frac{\partial \rho_j}{\partial E_j} \right)_P \frac{dE_j}{dQ} + \left(\frac{\partial \rho_j}{\partial P} \right)_{E_j} \frac{dP}{dQ} \right) &= 0, \\ \left(1 - \frac{P}{\rho_i(P, E_i)^2} \left(\frac{\partial \rho_i}{\partial E_i} \right)_P \right) \frac{dE_i}{dQ} - \frac{P}{\rho_i(P, E_i)^2} \left(\frac{\partial \rho_i}{\partial P} \right)_{E_i} \frac{dP}{dQ} &= \frac{\varepsilon_i}{m_i}, \end{aligned} \right. \quad (4)$$

where ε_f , ε_b – parts of the energy absorbed in HS components; x_f , x_b – mass concentrations of a filler and binder.

Pressure is used in (4) as a required variable instead HS components densities that differs from the general approach to creation of an elementary hydrodynamic cell [1]. Such choice of required variables allows to reduce number of unknown functions because pressures being formed in all HS components of a cell are assumed by the equal. Besides pressure introduction in a set of required functions is convenient at creation of the equation of a state for a polydisperse filler. This equation most simply turns out in the form $\rho_f = \rho_f(P, E_f)$ required for calculation of coefficients in equations system (4). But at such approach the creation of binder equation of states (EOS) is required also in the corresponding variables. It is some difficulty because density and internal energy are accepted to independent variables in caloric EOS widely used in practice. We note that the rupture of the first type appears in isotherms $\rho_b = \rho_b(P)$ for two-phase region and it is inconvenient generally.

Pressure P_0 and specific energy E_{f0} , E_{b0} for HS components before radiation (at $Q=0$) are taken as entry conditions for the received system of the equations (4):

$$P(0) = P_0, E_f(0) = E_{f0}, E_b(0) = E_{b0}. \quad (5)$$

The equations of a condition of a polydisperse filler are defined in the assumption that MS are thin elastic two-layer shells. These covers collapse as a result of dynamic loss of stability or exhaustion of bearing ability. Microspheres having small relative thickness

δ/r collapse on by means of stability loss. Microspheres having big relative thickness collapse by means of durability loss. Relationship between MS wall thickness δ and its radius r is defined from a condition of constancy of glass mass containing in various MS

$$N = \frac{3}{4\pi\rho_{cov}} \left[\int_0^\infty (r^3 - (r - \delta_{cov})^3) f(r) dr \right]^{-1},$$

where m_{cov} – mass part of a dusting containing in a filler; δ_{cov} – dusting thickness; ρ_{gl} – density of porous MS glass. The number N of filler MS containing in unit of mass is determined by a formula (ρ_{cov} – density of a porous MS dusting)

$$\frac{1 - m_{cov}}{N\rho_{gl}} = \frac{4\pi}{3} ((r - \delta_{cov})^3 - (r - \delta_{cov} - \delta)^3).$$

Filler EOS is defined from a relationship (6) when MS thickness and particles density N are known

$$\rho_f^{-1}(P, E_f) = N \int_0^\infty V_{MC}(r, P, E_f) f(r) dr, \quad (6)$$

where $V_{MS}(r, P, E_f)$ – the specific volume of the MS, compacted by pressure P and heated as a result of increase internal energy E_f . Volume containing between MS isn't included in a relationship (6) because it is filled with HS binder (i.e. mass per unit of volume of walls and internal MS cavities is understood as filler density).

The volume filled by multilayered MS having radius r is calculated in the assumption of her elastic behavior until to strength or stability loss

$$V_{MS} = \frac{4\pi}{3} r^3 \left[1 + 3\alpha_f(T_f - T_0) - \frac{P}{K_f} \right],$$

$$K_f = \frac{2}{3r} \sum_{j=gl,cov} \frac{E_j^f(T_f)\delta_j(r)}{1 - \nu_j}, \quad \alpha_f = \frac{2}{3rK_f} \sum_{j=gl,cov} \frac{E_j^f(T_f)\delta_j(r)\alpha_j(T_f)}{1 - \nu_j},$$

where E_j^f , ν_j , α_j – Young's modules, Poisson's coefficients and linear coefficients of temperature expansion of porous MS materials; α_f , K_f – effective coefficient of linear temperature expansion and coefficient of volume compression of a microspherical filler. Filler temperature T_f is calculated when temperature manages to become equal in MS limits because of its small thickness and when MS destruction precedes phase transitions

$$\int_{T_0}^{T_f} (m_{cov}c_{cov}(T) + (1 - m_{cov})c_{gl}(T))dT = E_f - E_{f0},$$

where c_{cov} , c_{gl} – specific thermal capacities of a dusting and MS material.

Volume of collapsed MS is supposed equal to the walls volume. Further change of volume is defined by means of EOS corresponding to continuous materials.

Dependence of density of a microspherical filler on pressure is given in fig. 5. Dependence is constructed by the considered method for the normal law of MS distribution on radius. This law has the center $\bar{r} = 25\mu\text{m}$ and various average quadratic deviations ($\sigma_r = 1; 3; 5 \mu\text{m}$).

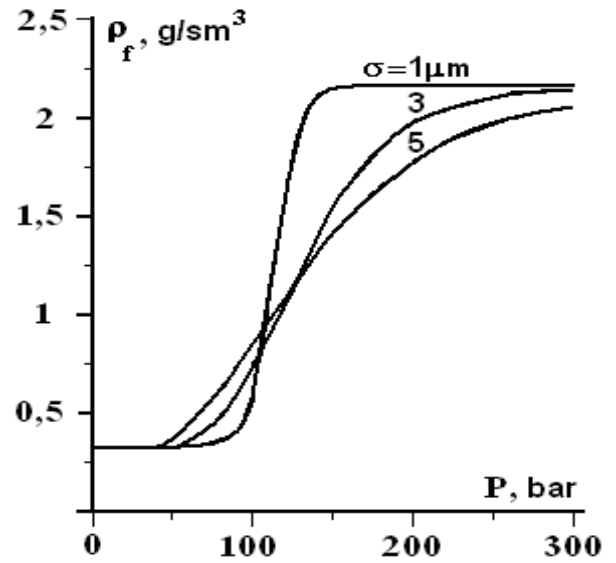


Fig. 5. Dependence of density of a microspherical filler on pressure

At first big and thin MS collapse when pressure increases. Such MS are present at HS having a wide variation of filler radius. Therefore curves settle down above at the initial stage of loading if σ_r is more (curve $\sigma_r = 5\mu\text{m}$ is higher than curves $\sigma_r = 1; 3\mu\text{m}$). But the situation changes on opposite when pressure becomes more because HS having a wide variation of filler radius contain many small MS. Small MS collapsed and condensed worse. (in this case curve $\sigma_r = 5 \mu\text{m}$ is below than curve $\sigma_r = 1; 3\mu\text{m}$). Shittings having a small variation ($\sigma_r = 1\mu\text{m}$) of filler radius collapse at nearest values of pressure and considered dependence is similar to theta-function.

The system of the differential equations (4) having entry conditions (5) and constructed EOS of a filler and binder decided by a

numerical method (Runge and Kutta's method having the fifth order of approximation and an automatic choice of integration step).

Dependences of initial pressure being formed in hypermarket from the specific absorbed energy at $\sigma_r = 1, 3, 5 \mu\text{m}$ are shown in

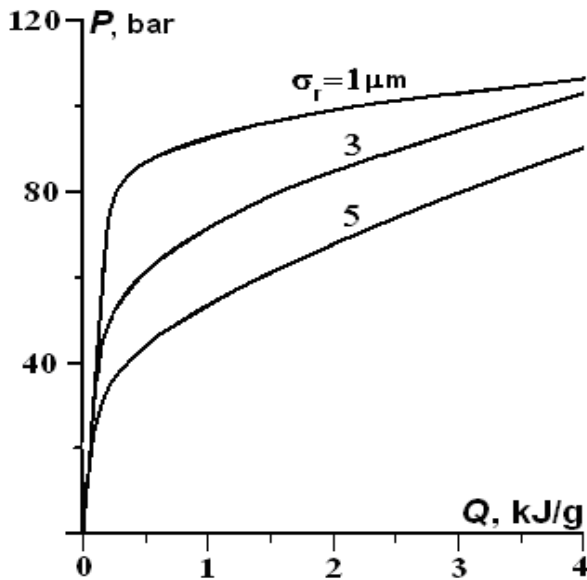


Fig. 6. Dependence of pressure P being formed in a cell from the specific absorbed energy Q

fig. 6. It is visible that all curves approach with increase in a power supply because after MS destruction the further HS behavior doesn't depend any more on the law of distribution of microspheres by the sizes. After completion of MS destruction the speed of pressure change increases in process of a supply of energy Q because HS compressibility significantly decreases. As a result the shelf of MS destruction is formed on dependence of pressure on energy release.

The offered models of elementary HS cells and the received results can be used for design of protective HS of the new generation working in the conditions of pulse volume absorption of high-intensity RPF. These models are applicable in conditions under which destruction of microspherical fillers takes place.

3.3 Thermal RPF action

Charging and thermal RPF actions are characterized by effect accumulation from influence to influence and have also complex nature of the processes providing construction

damage. Therefore the corresponding settlement models [10] are created for the general case of repeated RPF influence. These models have to be necessarily nonlinear (complexity is realized only in nonlinear models).

RPF interaction with composite materials can cause various physical and chemical transformations (PCT). The set of PCT changes upon transition from one rather narrow class of composite materials to another [11-17]. Usually heat-physical properties of binder and the filler strongly differ. Therefore nature of their thermal destruction will be also essential various. It is clear that for composite materials the mathematical model has to consider heterogeneous structure. In particular the model of a layered composite [10,15,17] is such model. Two sources of lamination are available in this model. The first source is the constructional. Construction packages consist of the diverse materials being various layers of model. The second source is the physical. Filler and binder of a composite material are the diverse layers having different natures of destruction. The uniform material is stratified on layers upon transition of its part to other phase state.

The equation of transfer of condensed phase energy is written taking into account PCT for each layer of a material [11,12,15] (the layer index is counted out)

$$\rho_s c_s \frac{\partial T}{\partial t} = \frac{\partial}{\partial x} \left(\lambda_{\Sigma} \frac{\partial T}{\partial x} \right) - G_g c_g \frac{\partial T}{\partial x} + \rho_s \left[\frac{dQ}{dt} + \sum_{k=1}^N U_k f_k(x) \delta(t-t_k) + \frac{dQ_{\text{pct}}}{dt} \right], \quad (7)$$

where T – temperature of a condensed phase of a layer and of gaseous products flowing on it; ρ_s, c_s – effective density and thermal capacities of layers; λ_{Σ} – total coefficient of molecular and radiation (in a time of a firm phase) heat conductivity; G_g, c_g – the values of a mass flux and a thermal capacity of gaseous products; dQ/dt – power of specific energy released at volume RPF absorption; $f_k(x)$ – spatial distribution of the given specific energy released to volume and instant (in particular time of influence of an IR impulse is significantly less than time of transmission of energy by heat conductivity and by convective transfer of gaseous products); k – influence number; U_k, t_k – radiation impulse and time of

k-influence of RPF; $\delta(t)$ – delta function; dQ_{pct}/dt – power of specific inflow (drain) of heat caused by RPF.

The sum containing in the right side of the equation (7) considers recurrence of RPF influences having volume nature of absorption and an instant supply of energy. The task of sequences $t_k, U_k, Q_k(x)$ allows to model any temporary sequence of any number of pulse influences.

The gas flux G_g caused by decomposition of binder is calculated approximately. It is supposed that all gas mass formed until considered section in the depth of a material flows with a small speed through this section. Distribution of normalized (on unit of area density of RPF energy) specific energy release $f_k(x)$ is calculated by statistical methods of modeling of RPF transfer (see section 3.1). Inflow (drain) of heat in a material as a PCT result dQ_{pct}/dt is defined by total thermal effect of the corresponding transformations.

Three groups of boundary conditions are considered generally.

1. Conditions formulated on irradiated boundary

a) PCT boundary moving with a speed D ($\gamma_m=0$)

$$\lambda_x \frac{\partial T}{\partial x} = q_{Li}(t) + q_{con}(t) - \frac{\varepsilon(T)}{\alpha_p} \sigma_{SB} T^4 - \rho_s D \left[\Delta H + \frac{(D+u)^2 - D^2}{2} \right] + \gamma_m \frac{\partial T}{\partial t}, \quad (8)$$

where $\Delta H = E_g + P_g / \rho_g - H_s$ – a difference of specific enthalpies of condensate and gas products of PCT (P_g, E_g, ρ_g – pressure, specific internal energy and density of gaseous products of an ablation respectively); u – speed of gaseous products; q_{Li} – stream of the radiation absorbed superficially on boundary; q_{con} – convective thermal flux; $\varepsilon(T)$ – integrated radiation coefficient; σ_{SB} – Stefan-Boltzmann constant; γ_m – the coefficient depending on T ; $\alpha_p = \rho_s(0) / \rho_s(t)$ – current porosity of composite.

b) boundary without PCT – a condition (8) with $D = 0, \gamma_m = 0$.

c) boundary from thin protective (well reflecting PICH) layer of "metal" (any material having high heat conductivity and small thickness) – a condition (8) with $D = 0$ and $\gamma_m = \rho h c_m(T)$ (ρ, c_m, h – density, a thermal capacity and thickness of a "metal" layer).

2. Conditions formulated on boundary between i and $i+1$ layers

a) PCT boundary moving with a speed D ($\gamma_m = 0$)

$$T_i = T_{i+1}, \quad \lambda_{\Sigma, i+1} \frac{\partial T_{i+1}}{\partial x} - \lambda_{\Sigma, i} \frac{\partial T_i}{\partial x} = \rho_m D \Delta H + \gamma_m \frac{\partial T_i}{\partial t} + q_i^* \quad (9)$$

where ρ_m – density of a layer material that has PCT; ΔH – a difference of enthalpies of PCT products and an initial material; q_i^* – RPF flux absorbed on boundary.

b) contact boundary – a condition (9) with $D = 0, \gamma_m = 0$;

c) boundary having a metal parting – a condition (9) with $D = 0, \gamma_m = \rho h c_m(T)$.

3. Conditions formulated on back boundary

a) PCT boundary moving with a speed D

$$-\lambda_x \frac{\partial T}{\partial x} = q_R(t) + q_{con}(t) - \frac{\varepsilon(T)}{\alpha_p} \sigma_{SB} T^4 - \rho_s D \left[\Delta H + \frac{(D+u)^2 - D^2}{2} \right], \quad (10)$$

b) boundary with convective and radiation streams generated by high-temperature mix of gases – condition (10) with $D = 0$

c) radiating boundary without supply of thermal fluxes – a condition (10) with $D = 0, q_{con}(t) \equiv q_R(t) \equiv 0$.

d) the heat-isolated boundary – a condition (10) with

$$D = 0, \lambda_x \equiv -1, q_{con}(t) \equiv q_R(t) \equiv 0, \varepsilon(T) \equiv 0.$$

Thus the equations of transfer of thermal condensed phase energy added with boundary and initial conditions allow to consider the following main sources (drains) of thermal energy: external convective supply of heat from a running air flux; internal convective supply of heat from the high-temperature mix of gases flowing through an element; heat supply of radiant streams from radiating gas; radiant supply of heat at superficial absorption of radiation; heat supply in case of repeated instant volume radiation absorption; energy drain because of thermal radiation from surfaces of a heated construction; PCT energy costs occurring on boundaries.

It is visible from the given equations that each group of boundary conditions is reduced to the first of them. Numerical realization of a heat problem becomes simpler when all almost important boundary situations are expressed through three main boundary conditions.

The formulated problem is solved by a method of finite differences [18] by means of the implicit scheme [15,17]. In relation to a considered problem search of the numerical decision becomes complicated that boundary conditions are set on moving PCT. Boundaries locations are unknown in advance and are defined during calculation of a temperature field. The immovability of boundaries of each layer is reached by variables replacement at which barrier layers of a are imaged on intervals (0,1) [15].

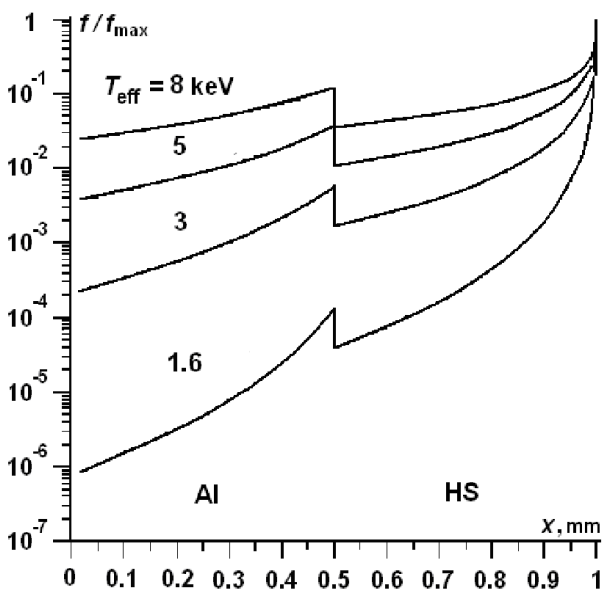


Fig. 7. Profiles of IR energy releases for Plank's spectrum $T_{\text{eff}}=1,6; 3; 5; 8 \text{ keV}$

The system of the algebraic equations received by finite-differential method is solved by means of an iterative Newton's method. Running method is used for the solution of three-diagonal system of the linear equations received on each step of iteration. Performance of the law of energy conservation is checked in the course of calculations. It is made for additional control of stability and calculation accuracy. Testing was held for the problems having the analytical solution [19]. Such testing adds confidence of a correctness of numerical algorithm and programs realizing model of

heating and thermal destruction of composite materials at repeated RPF influence. The deviation of the numerical results from the analytical solution didn't exceed 0,1% in all considered test problems.

As a settlement example repeated IR influence having volume and instant energy release is considered on a two-layer target (carrier layer made from aluminum and a protective HS layer made from fiberglass plastic with thickness: 0,5+0,5sm). It is supposed that streams of AI have Plank's spectrums characterized by effective temperatures: 1,6 (soft spectrum), 3, 5, 8keV (rigid spectrum). Methods of IR transfer modeling presented in section 3.1 allow to receive profiles of energy releases. These profiles are given in fig. 7 for all considered spectrums. It is visible that energy release has big gradients localized in the field of an irradiated surface. Therefore the fiberglass plastic layer breaks on thin near-surface layer having thickness 0,01sm and the rest layer having thickness 0,49sm (the target was considered as three-layer with thickness 0,5+0,49 +0,01sm) for providing of demanded accuracy (about several degrees, i.e. the error of calculation shouldn't exceed 0,1%) of definition of temperature profiles.

Four influences having time points of $t = 0, 3, 6, 9\text{s}$ are considered. Apparently time intervals between these influences are equal. It is supposed that heating matters only until $t = 12\text{s}$. This time makes sense of duration of functioning of studied object. Duration is counted from the beginning of the first influence.

Temperatures reached in a target at four IR influences with increase of rigidity of spectrum (1,6 + 3 + 5 + 8keV – a dashed line) and its decrease (8+ 5 + 3 + 1,6keV - the thick line) are shown in fig. 8,9. Fixed energy density took place in each impulse was equal $10\text{J}/\text{sm}^2$. Spatial profiles are presented for the time moments of completion of influences and to the end of object functioning. Spatial coordinate is normalized on thickness of layers. Then the maximum number 3 shown on ordinate axis of

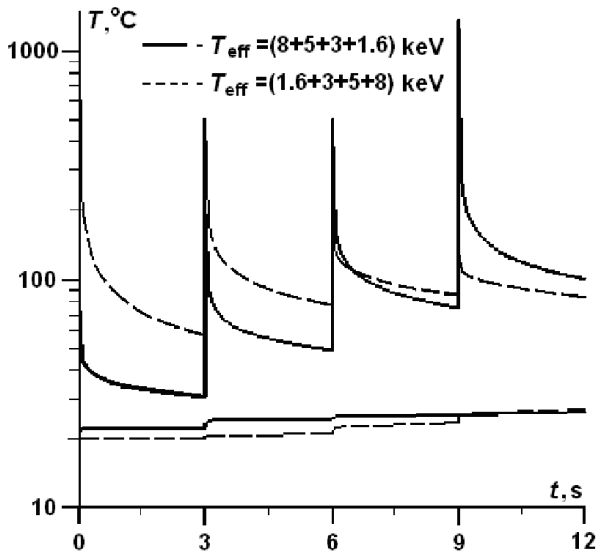


Fig. 8. Change of temperatures of target surfaces at four IR influences

figure 9 corresponds to consideration of a three-layer target.

It is visible that temperatures difference at various sequences of influences is insignificant by the time $t = 12$ s. The sequence having final soft spectrum (this spectrum gives the greatest gain of temperature) leads to more high final

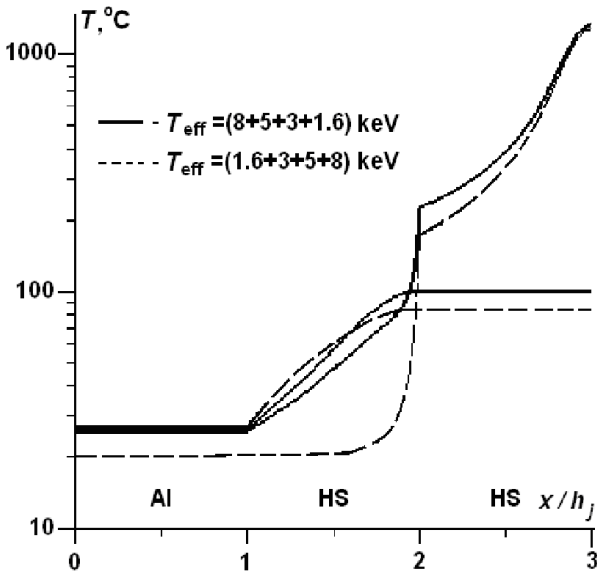


Fig. 9. Spatial temperature profiles at four IR influences

temperature near an irradiated surface. Temperature has less time for the reduction on means of radiation from a surface and of heat redistribution in a target. The situation is the return in a carrier layer. This layer is warmed

more strongly at early influence of a soft range. In this case heat has big time for redistribution in target depth.

3.4 Charging RPF action

Models of charge accumulation and electric fields formation realized in dielectrics at RPF influence were considered in many works [20-30]. Rather simple model of calculation of electric fields which are formed in multilayered flat packages of construction at joint action of neutral energy fluxes (gamma-X-ray radiation and neutrons) is used in the present work. Known macroscopic characteristics of materials are included in the mathematical formulation of this model. This fact is advantage of considered model.

It is supposed that the size of radiation area considerably exceeds target thickness. Then the problem is one-dimensional. In this case electric field E_x being formed in each of N layers having dielectric permeability $\epsilon_{el k}$ is defined from Maxwell's one-dimensional equation ($k=1, \dots, N$)

$$\epsilon_{el k} \epsilon_0 \frac{\partial E_x}{\partial x} = \rho_{el}(x, t), \quad (11)$$

where $\epsilon_0 = 8,85 \times 10^{-12}$ F/m – dielectric permeability of vacuum; x – distance from an irradiated surface measured along a normal to a target; $\rho_{el}(x, t)$ – distribution of volume density of a charge on target thickness for time t .

The superficial charge $\sigma_{el k+1}(t)$ is formed on boundaries localized between layers k and $k+1$ as a result of violation of electronic balance. Value of electric field jump depends on the size of this charge ($k=1, \dots, N$)

$$\Delta E_{xk+1} = E_x(x_{k+1} + 0, t) - E_x(x_{k+1} - 0, t)$$

$$(E_x(x_{k+1} - 0, t) + \Delta E_{xk+1}) \epsilon_{el k+1} - E_x(x_{k+1} - 0, t) \epsilon_{el k} = \sigma_{el k+1}(t) / \epsilon_0, \quad (12)$$

where x_k, x_{k+1} – the coordinates of boundary of k -go of a k -layer ($x = x_1 = 0$ – the coordinate of an irradiated surface).

It is necessary to formulate one more condition relating to external boundaries for uniqueness of the solution of the equation (11). This condition is additional to conditions (12) for multilayered packages formulated on internal boundaries. Various schemes of

irradiation and the corresponding boundary conditions are considered [27] rather in detail. It is advisable to consider two types of boundary conditions in relation to a considered case of influence of electrically neutral RPF (gamma and x-ray radiation and neutrons) acting on AC constructions. The total target charge remains equal to zero (for simplicity lack of carrying out of electrons from an irradiated surface is supposed in model) at influence of neutral fluxes. Then the additional boundary condition is formulated similarly (12)

$$\Delta E_{x1} = E_x(0+0, t) = \frac{\sigma_{el1}(t)}{\varepsilon_0 \varepsilon_{el1}}. \quad (13)$$

We receive from (11)-(13) because the total charge of a target is equal to zero

$$E_x(h+0, t) = \int_0^h \rho_{el}(x) dx + \sum_{k=1}^{N+1} \sigma_{elk} = 0.$$

This result follows also from Gauss's theorem.

But other approach is possible. The irradiated near-surface layer and other layers of a package have high conductivity. In this case the boundary condition of short circuit along end faces of a construction is correct. Then the condition of a zero potential difference is written out as

$$\int_0^h E_x(x, t) dx = 0, \quad (14)$$

where h – full thickness of a multilayered package.

Use of two various conditions (13) and (14) at the solution of the same problem allows to estimate interval of changes of electric fields in intermediate cases of partial alignment of a potential difference between irradiated and back boundaries of a construction.

The knowledge of distributions of superficial $\sigma_{elk}(t)$ and volume $\rho_{el}(x, t)$ charges is required for the solution of the equation (11) together with boundary conditions (12) and (13) or (14). These distributions can be found from the equations of a continuity of currents ($\gamma_\Sigma(x, t, E_x)$ – distribution of conductivity of the environment).

$$\frac{\partial \rho_{el}}{\partial t} = \frac{\partial j_e}{\partial x} - \frac{\partial}{\partial x} [\gamma_\Sigma(x, t, E_x) E_x], \quad (15)$$

$$\frac{d\sigma_{elk}(t)}{dt} = [j_e(x, t)]_{x_{k-1}+0}^{x_k+0} - [\gamma_\Sigma(x, t, E_x) E_x(x, t)]_{x_{k-1}+0}^{x_k+0}, \quad (16)$$

if density of electrons currents $j_e(x, t)$ are known. It should be noted that the value $j_e(x, t)$ is

considered positive in (15) and (16) when electrons move in the positive direction of an axis x .

Conductivity of materials consists of own (dark) conductivity $\gamma_{dark}(E_x)$ and radiation conductivity $\gamma_{rad}(E_x)$, acquired as a result of influence

$$\gamma_\Sigma = \gamma_{dark}(E_x) + \gamma_{rad}(E_x). \quad (17)$$

As a first approximation radiation conductivity γ_p is considered proportional to powers of doses of radiations and neutrons. Sedate dependence [25] is more general. But as a rule the exponent is unknown (it changes from 0,5 to 1) and use of linear dependence is represented admissible. Besides we consider that each of influencing factors acts independently. Then we receive from (17)

$$\begin{aligned} \gamma_\Sigma &= \gamma_{dark0} + (\gamma_{rup} - \gamma_{dark0}) \times f_{rup}(E_x) + \\ &K_n(dQ/dt)_n + K_\gamma(dQ/dt)_\gamma + K_p(dQ/dt)_p, \\ f_{rup}(E_x) &= \begin{cases} 0, & |E_x| \leq k_{rup} E_{rup}, \\ \left(\frac{|E_x|/E_{rup} - k_{rup}}{1 - k_{rup}} \right)^{\alpha_{rup}}, & k_{rup} E_{rup} < |E_x| \leq E_{rup}, \end{cases} \end{aligned} \quad (18)$$

where $K_{n,\gamma,p}$ – proportionality coefficients. It is supposed in relationship (18) that near values of electric breakdown field E_{rup} the deviation from the Ohm's law can be described by sedate dependence [25,31]. This dependence contains three constants of a material. There are conductivity after breakdown γ_{rup} , exponent α_{rup} and coefficient k_{rup} ($0,95 < k_{rup} < 1$).

Thus system of the equations (11), (15), (16) together with boundary conditions (12)–(14) and zero entry conditions ($k=1 \dots N+1$)

$$E_x(x, 0) = 0, \quad \rho_{el}(x, 0) = 0, \quad \sigma_{elk}(x, 0) = 0 \quad (19)$$

allows to determine density of volume and superficial charges and electric fields localized in multilayered construction packages if functions of electrons currents $j_e(x, t)$ and power of doses $(dQ/dt)_n, (dQ/dt)_\gamma, (dQ/dt)_p$ are set.

Non-stationary functions required for calculations are defined from the calculated stationary distributions received by a statistical method (see section 3.1)

$$\begin{aligned} \frac{\partial j_e(x, t)}{\partial x} &= \frac{\partial i_n(x)}{\partial x} q_n(t) + \frac{\partial i_\gamma(x)}{\partial x} q_\gamma(t) + \frac{\partial i_p(x)}{\partial x} q_p(t), \quad (20) \\ (dQ/dt)_{n,\gamma,p} &= f_{n,\gamma,p}(x) q_{n,\gamma,p}(t), \end{aligned}$$

where $q_{n,\gamma,p}(t)$ – fluxes of the corresponding type of considered RPF; $i_{n,\gamma,p}(x)$ – stationary profiles of current of secondary electrons for single impulses of the corresponding RPF. Representation (20) of basic data required for a considered problem is very conveniently because functions $f(m)$, $i_{n,\gamma,p}(m)$ entering in representation (20) are characteristics of materials of a studied multilayered package. These functions don't depend on temporary distributions of impulses of influencing RPF. But these functions oscillate because the statistical method is used for their calculation. Existence of oscillations is inadmissible for further use in calculations based on a finite difference method. Creation of smooth approximations of statistical data is an exit from this difficulty. Approximating functions undertake identical to all types of influences

$$i_{n,\gamma,p}(x) = a_{n,\gamma,p} + b_{n,\gamma,p}x + c_{n,\gamma,p} \exp(-d_{n,\gamma,p}x),$$

$$f_{n,\gamma,p}(x) = A_{n,\gamma,p} + B_{n,\gamma,p}x + C_{n,\gamma,p} \exp(-D_{n,\gamma,p}x).$$

Finite difference method is used for the solution of a problem (11), (12), (14), (15), (16), (19). The multilayered package breaks into cells having the equal size $\Delta x = (x_{k+1} - x_k) / N_k$ for each layer k . One of boundaries of extreme cells coincides with the corresponding boundary of a layer (N_k – number of splittings in layer k). Density of a volume charge ρ_{el} and divergency of density of electrons currents $\partial j_e(x,t) / \partial x$ are set in the centers of cells. Other values are defined on cell boundaries. The implicit scheme [18] having the second order of accuracy on temporary and spatial variables is used [10] (the wave located over a variable means that it is calculated from values on the previous iteration; $\gamma_{\Sigma 0} = \gamma_{\Sigma N+1} = 0$; $\varepsilon_{el0} = \varepsilon_{elN+1} = 1$):

for $k = 1, \dots, N$

$$\frac{E_{xi+1}^{n+1} - E_{xi}^{n+1}}{\Delta x_k} = \frac{\rho_{eli+1/2}^{n+1}}{\varepsilon_{elk} \varepsilon_0}, \quad (21)$$

$$2\Delta x_k \frac{\rho_{eli+1/2}^{n+1} - \rho_{eli+1/2}^n}{\Delta t} = 2\Delta x_k \left(\frac{\partial j_e(x,t)}{\partial x} \right)_{i+1/2}^{n+1/2} - (\gamma_{\Sigma i+1}^n E_{xi+1}^n - \gamma_{\Sigma i}^n E_{xi}^n) - \left\{ \left[\gamma_{\Sigma i+1}^{n+1} + \left(\frac{d\tilde{\gamma}_{\Sigma}}{dE_x} \right)_{i+1}^{n+1} \right] E_{xi+1}^{n+1} - \left(\frac{d\tilde{\gamma}_{\Sigma}}{dE_x} \right)_{i+1}^{n+1} (\tilde{E}_{xi+1}^{n+1})^2 - \gamma_{\Sigma i}^{n+1} E_{xi}^{n+1} \right\},$$

for $k = 1, \dots, N + 1$:

$$(E_{xi_k}^{n+1} + \Delta E_{xk}^{n+1}) \varepsilon_{elk} - E_{xi_k}^{n+1} \varepsilon_{elk-1} = \frac{\sigma_{elk}^{n+1}}{\varepsilon_0},$$

$$2 \frac{\sigma_{elk}^{n+1} - \sigma_{elk}^n}{\Delta t} = 2 [\Delta j_e(x,t)]_k^{n+1/2} - \left\{ \gamma_{\Sigma k}^{n+1} + \left(\frac{d\tilde{\gamma}_{\Sigma}}{dE_x} \right)_k^{n+1} (\tilde{E}_{xi_k}^{n+1} + \Delta \tilde{E}_{xk}^{n+1}) \right\} (E_{xi_k}^{n+1} + \Delta E_{xk}^{n+1}) - \left(\frac{d\tilde{\gamma}_{\Sigma}}{dE_x} \right)_k^{n+1} (\tilde{E}_{xi_k}^{n+1} + \Delta \tilde{E}_{xk}^{n+1})^2 - \gamma_{\Sigma k-1}^{n+1} E_{xi_k}^{n+1} + \gamma_{\Sigma k}^n (E_{xi_k}^n + \Delta E_{xk}^n) - \gamma_{\Sigma k-1}^n E_{xi_k}^n,$$

where i_k, i_{k+1} – boundaries indexes of a layer k .

The system of finite difference equations (21), (22) solves by an iterations method on each temporary step. During iterations running is realized from external irradiated boundary where field value E_{x1}^{n+1} is set by a boundary condition (13) and area density of a charge σ_{el1}^{n+1} is defined from the second equation (22) at $k=1$. During running from i point to $i+1$ point new values of charge density located in a point $i+1/2$ and electric field located in a point $i+1$ are defined from the equations (21) considered as linear system of two equations relatively $\rho_{eli+1/2}^{n+1}$ and E_{xi}^{n+1} . The analytical decision of this system is used in numerical algorithm. Values of electric field \tilde{E}_{xi+1}^{n+1} undertake from results of the previous iteration. These values are accepted equal to the corresponding values E_{i+1}^n on the previous temporary layer n at the first iteration. Value of conductivity and its derivative on field are calculated on the set fields of energy release by means of relationships (18). The equations (22) are used on layers boundaries for calculation of values of surface charge density σ_{elk}^{n+1} and electric field $E_{xi_k}^{n+1} + \Delta E_{xk}^{n+1}$ localized to the right of boundary. Value of a electric field $E_{xi_k}^{n+1}$ localized at the left of boundary is already known as a result of the previous step of running. The equations (22) are considered as linear system two equations as before. After running completion new iteration becomes until the next condition will be satisfied

$$max_i (|E_{xi}^{n+1} - \tilde{E}_{xi}^{n+1}|) < \delta_{rel} |\tilde{E}_{xi}^{n+1}| + \delta_{abs},$$

где $\delta_{rel} \approx 10^{-5}$, $\delta_{abs} \approx 10^{-8}$ – заданные точности итераций.

The boundary condition (14) can also be realized in numerical algorithm. In this case the

received field is corrected on each iteration on a formula

$$(E_{xi}^{n+1})_{cor} = E_{xi}^{n+1} - \int_0^{\delta_{\Sigma}} E_x(x, t^{n+1}) dx / \left(\varepsilon_{elk} \sum_{j=1}^N \delta_j / \varepsilon_{elj} \right), \quad (23)$$

where δ_j – thickness of layers

($\delta_{\Sigma} = \sum_{j=1}^N \delta_j$). where δ_j – thickness of layers ().

The integral containing in a formula (23) is defined by trapezes method for values E_{xi}^{n+1} of discrete distribution of electric field.

Results of calculations made on offered numerical model are presented in [10].

4 Experimental verification of strength

The numerical solutions of problems of constructions strength are insufficient at creation of modern AC. Experimental test are the main method of confirmation of strength of the responsible AC elements. These tests are carried out on the basis of gasdynamic devices of reproduction of RPF actions and imitators of trajectory heat-force loadings.

The analysis of mechanical RPF action at various change ranges of waves lengths representing practical interest, of fluxes density, of external conditions and target materials properties is carried out in [2,32]. This analysis allows to formulate requirements to loadings characteristics which need to be reproduced at modeling mechanical RPF action. Need of development of devices which generate loadings having durations $\tau_p = 0,01...300 \mu s$ and pressure impulses $I_p = 0,02...5 \text{ kPa}\times s$ follows from these requirements. The set of explosive gasdynamic devices allowing to model mechanical RPF action taking place on large-size thin-walled AC constructions is offered in [32] for various RPF energy spectrums representing practical interest. Need of generation of loadings having various space-time distributions was taken into account at creation of these devices. The set of gasdynamic devices allows to reproduce loadings having durations $\tau_p = 0,2...500 \mu s$ and pressure impulses $I_p = 0,05...5 \text{ kPa}\times s$. These loadings characteristics short conform to requirements imposed to devices to modeling RPF action. Creation of the gasdynamic devices generating low-pulse and ultrashort loadings

having $I_p \leq 0,05 \text{ kPa}\times s$ and $\tau_p \leq 0,2 \mu s$ is necessary. Some reduction of pressure impulse can be still reached by modernization of light-detonating explosive charge [2]. But the problem of duration reduction is insoluble if we are limited to a framework of a gasdynamic method. It seems that this method exhausted the capabilities. We will hope for creation of methods of loadings generation using physical processes other than a explosives detonation. In particular low-pulse and ultrashort loadings can be created by means of electric explosion of foils [33] or influence of electron beams [34].

Need of an assessment of AC elements strength taking place at action of non-stationary loadings arises long before their creation. Verification of strength is required already at a steps of designing and a choice of the most optimum constructive solutions. But composite materials widely applied in SC don't exist separately from a construction. These materials are created together with a construction in the same technological process. Therefore generally speaking the experimental test of material strength is possible only after making of construction [35]. Nevertheless it is preferable to investigate strength of fragments and to carry out some finishing tests of construction at a final stage. Such choice of a research method is explained by the following reasons. First the cost of a composite construction is significantly more in comparison with its fragments. As a rule one composite construction (for example high pressure shell made by a method of cotton winding) can be fragmented on a set of the same elements. Secondly there is a possibility of making of fragments having strength characteristics that are similar on characteristics of construction materials. It is essentially that fragments are produced without construction creation. Thirdly devices of generation of low-pulse and short loadings are absent for surfaces having the characteristic sizes of AC constructions.

Non-stationary loadings are conditionally subdivided on pulse or dynamic. This division is made in dependence of features of loadings action and the reasons of construction damage. Conditions of dynamic loading are realized in a case when action duration is comparable with a

period of free vibration of thin-walled construction. It is also necessary that time of acoustic indignation propagation took place on thickness is more loading duration at 10-15 times. Last condition provides prevalence of shell stage of deformation. Destruction of AC construction elements is realized owing to development of inadmissible deflections and formation of cracks if loadings are dynamic.

Pulse loading takes place when duration of action doesn't exceed a quarter of a period of free shell vibration. If loading duration appears also less time of acoustic indignation propagation then the main destruction cause is a development of wave processes. Wave processes are accompanied by formation of stratifications (it is characteristic for a composite) and spall fractures. But process of deformation will be transformed to shell stage if pulse loading acts on thin-walled constructions. Stress waves damp and their spatial size increases to the sizes of construction thickness. After that time non-stationary processes are realized as shell movement. Application of damping sheetings reduces a role of wave processes for construction fracture. But these sheetings don't protect from development of inadmissible deflections and formation of cracks. The example of construction fracture as a result of shell deformation is presented in fig. 10. Non-stationary circular deformations reached 1% in the region of a loading center.

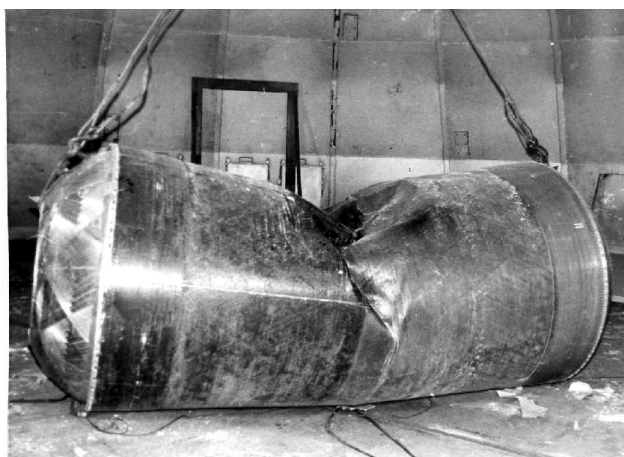


Fig. 10. Consequences of dynamic loading ($I_p = 0,5\text{kPa}\times\text{s}$, $\tau_p = 100 \mu\text{s}$)

Axial deformations localized in the same region

exceeded 2%. The cover lost stability and the considerable dent was formed in a loading zone. Therefore finishing tests verifying strength of all construction to dynamic loadings are useful anyway. In particular it is necessary in an unevident case when actions of pulse character take place only.

Feature of the pulse loadings leading to wave destructions is locality of their action. Locality allows to cut out a fragment from a construction and to put it in such conditions at which destructions of a fragment and corresponding part of a construction are similar. In particular these destructions happen at

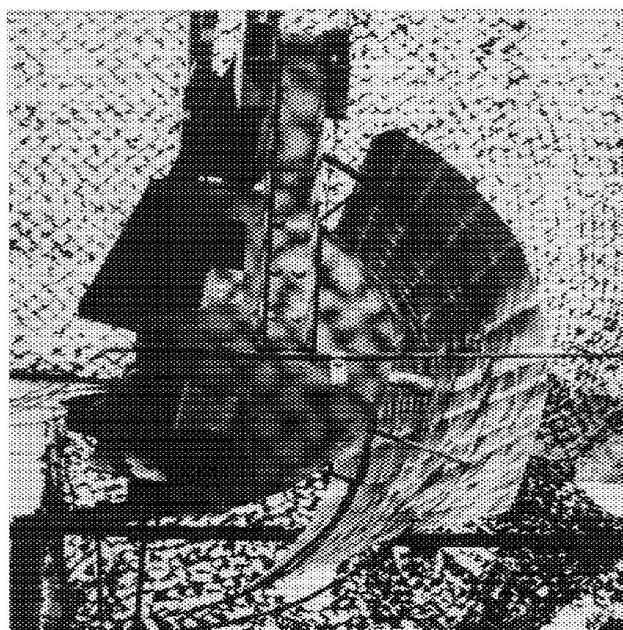


Fig. 11. Charge distributed equally from a surface

coinciding parameters of loadings.

Therefore it is represented expedient [36] to carry out two stages of tests of thin-walled designs to action of non-stationary and mechanical loadings being formed at RPF influence. Detailed research of wave processes and destructions caused by action of pulse loadings of fragments is carried out at the first stage. Finishing tests of all construction are made at the second stage in the conditions of its flight functioning and at influence of the dynamic loadings leading to shell deformation. Achievement of the second tests stage demands modeling of flight conditions together with reproduction of RPF actions. Some modeling devices which to be necessary for the second

stage are presented in [2,37]. As an example of the photo of two gasdynamic devices are

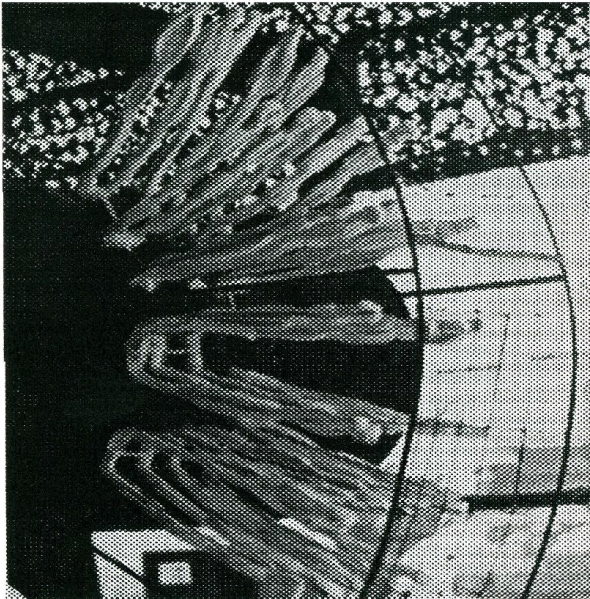


Fig. 12. Charge distributed on volume

presented in fig. 11, 12.

The described two-stage method of constructions test and set of devices reproducing non-stationary RPF actions and flight conditions were repeatedly used at strength verifications various types of AC elements [2, 38-40]. Working solid-fuel rocket engines were tested also [39].

Thus settlement and experimental forecasting of consequences of RPF actions located on AC constructions having heterogeneous sheetings demands development of methods of the solution of various physical problems. Now these problems are still far from completion. Drawing attention of young researchers to some problems considered only partially was the purpose of the present work.

References

- [1] Ostrik A.V. *Thermomechanical action of x-ray radiation on multilayered heterogeneous barriers in air*. Moscow, Scientific and technological center Informtechnics, 2003.
- [2] Bakulin V.N., Griбанov V.M., Ostriк A.V., et al. *Mechanical action of x-ray radiation on thin-walled composite constructions*. Moscow, Fizmatlit, 2008..
- [3] Griбанov V.M., Ostriк A.V., Romadinova E.A. Method of assessment of an energy release in components of sphere plastics irradiated by x-ray radiation taking into account energy redistribution by electrons. *Constructions from composite materials*, Issue 1, pp. 40-47, 2009.
- [4] Berger M.J. Reflection and Transmission of Gamma Radiation by Barriers: Monte Carlo Calculation by a Collision-Density method. *Journal of Research of the National Bureau of Standards*, Vol. 55, No. 6, pp. 343-350, 1955.
- [5] Lenchenko V. M. About electrization of bodies by γ -radiation. *Atomic energy*, Vol. 29, No. 1, pp. 53-55, 1970.
- [6] Ostriк A.V. Potapenko A.I. Calculation of effective Gruneisen coefficient at action on heterogeneous materials of pulse radiation. *Chemical physics*, Vol. 19, No. 2, pp. 23-26, 2000.
- [7] Anderholm N.C., Anderson Ph.D. Laser-Heating Studies of Composite Materials. *Journal of Applied Physics*, Vol. 43, No. 4, 1972.
- [8] Ostriк A.V. Ostriк E.A. Pressure calculation at impact of x-ray radiation on a heterogeneous material with the plastic binder. *Constructions from composite materials*, Issue 2, pp. 26-32, 1999.
- [9] Ostriк A.V. Two-dimensional model of a temperature and nonequilibrium elementary cell for protective heterogeneous coverings with a disperse filler. *Constructions from composite materials*, Issue 1(133), pp. 8-17, 2014.
- [10] Ostriк A.V., Griбанov V.M., Romadinova E.A. *Numerical code for calculation of repeated complex action of radiations and particles on a multilayered multipurpose heterogeneous flat package*. Chernogolovka, IPCP RAS, 2006.
- [11] Polezhayev Yu.V. Theoretical analysis of non-stationary warming up and fibreglass destruction in a vicinity of a critical point. *News of Academy of Sciences of the USSR, Mechanic and mechanical engineering*, No. 3, pp. 3-8, 1964.
- [12] Pankratov B.M., Polezhayev Yu.V. Rudko A.K. *Interaction of materials with gas fluxes*. Moscow, Mechanical engineering, 1976.
- [13] Polezhayev Yu.V., Yurevich F.B. *Thermal protection*. Moscow, Energy, 1976.
- [14] Shabunya S.I., Gusev V.S., Moyseenko L.G. et al. *Mathematical model of research of processes of interaction of a radiation thermal flux with composite materials*. Preprint No. 3, Institute of Lykov, AS BSSR, Minsk, 1985.
- [15] Ostriк A.V. Slobodchikov S.S. Mathematical model of destruction of composite shells of a high pressure under the influence of radiant fluxes of energy. *Mathematical modeling*, Vol. 7, No. 10, pp. 33-46, 1995.
- [16] Dimitriyenko Yu. I. *Mechanics of composite materials at high temperatures*. Moscow, Mechanical engineering, 1997.
- [17] Griбанov V.M., Ostriк A.V., Slobodchikov S.S. Thermal action of x-ray radiation on composite shells of a high pressure. *Constructions from composite materials*, Issue 2, pp. 18-28, 2002.

- [18] Godunov S. K., Ryabenky V.S. *Differential schemes*. Moscow, Science, Fizmatlit, 1973.
- [19] Lykov A.V. *Heat conductivity theory*. Moscow, the Higher school, 1967.
- [20] Murphy V.P. Gross B. Polarization of dielectrics by nuclear radiation. *Appl. Phys.*, Vol. 35, pp. 171-174, 1964
- [21] Gross B. Compton Current and Polarization in Gamma-Irradiated Dielectrics. *Appl. Phys.*, Vol. 6, No. 5, pp. 1635-1641. 1965.
- [22] Gromov V.V., Surikov V.V. Electric charge in radioactive dielectrics. *Atomic energy*, Vol. 32, No. 2, pp. 172-173, 1972.
- [23] Evdokimov A.B., Gusel'nikov V.N. Phenomenology model of accumulation of a volume charge in the dielectrics irradiated by fast electrons. *Chemistry of high energy*, No. 8, pp. 423-427, 1974.
- [24] Evdokimov O.B., Yalovich A.P., Shevelev G.E. Influence of electric field in dielectrics and semiconductors on an exit of Compton electrons. *Physics of a solid*, Vol.16, No.8, pp.2308-2399, 1974.
- [25] Gromov V.V. *Electric charge in the irradiated materials*. Moscow, Energoizdat, 1982.
- [26] Azernikova I.P., Mamonov M.N., Strikhanov M. N. Kinetics of accumulation and relaxations of an electric volume charge in the gamma-irradiated dielectrics. *The kinetic phenomena in semiconductors and dielectrics*, the Collection under Rudenko A.I. edition. Moscow, MIPhI, p. 34, 1985.
- [27] Boev S.G., Ushakov V.Ya. *Radiation accumulation of a charge in firm dielectrics and methods of its diagnostics*. Moscow, Energoatomizdat, 1991.
- [28] Sadovnichy D.N., Golub E.A., Tyutnev A.P., Yushkov A.V. Calculation of electric fields in flat heterogeneous structures. *Chemistry of high energy*. Vol. 29, No. 5, pp. 3-8, 1993.
- [29] Goncharov V.V., Kovalyov S.I., Kocce YU.V., Malkov S.Yu. Calculation of process of redistribution of electric charge in cylindrical dielectric constructions at influence of radiations and ionization heating. *Chemistry of high energy*, Vol. 29, No. 5, pp. 9-14, 1993.
- [30] Akishin A.I. Electrical breakdown of the dielectrics loaded radiation at imitation of influence of space radiations. *Perspective materials*, No. 3, pp. 5-15, 2005.
- [31] Vorobyov A.A., Zavadvosky E.K. *Electrical strength of solid dielectrics*. Moscow, GITTL, 1956.
- [32] Loborev V.M., Ostriak A.V., Petrovsky V.P., Cheprunov A.A. *Methods of modeling of mechanical action of radiations on materials and constructions*. Scientific and technical collection, No. 1, S. Posad, CPTI, 1997.
- [33] Burtsev V.A. Kalinin N. V., Luchinsky V.A. *Electrical explosion of conductors and its application in electro-physical installations*. Moscow, Energoatomizdat, 1990.
- [34] Boiko V. I., Skvortsov VA., Fortov V.E., Shamanin I.V. *Interaction of pulse bunches of the charged particles with substance*. Moscow, Fizmatlit, 2003.
- [35] *Mechanics of constructions from composite materials*. The collection of scientific articles under edition of V.D. Protasov, Moscow, Mechanical engineering, 1992.
- [36] Ostriak A.V., Petrovsky V.P. Experimental methods of research of operability of constructions from composite materials in the conditions of influence of non-stationary loadings. *Constructions from composite materials*, Issue 1, pp. 3-9, 1996.
- [37] Ostriak A.V., Bakulin V.N., Cheprunov A.A. Experimental methods of research of mechanical action of radiations on thin-walled composite cases of constructions. *Strength and plasticity problems*, Nizhny Novgorod, Publishing house of NNGU, No. 3, pp. 117-121, 2000.
- [38] Bakulin V.N., Ostriak A.V. Non-stationary deformation and destruction of composite covers. *News of the RAS*, Mechanics of solid, No. 4, pp. 135-142, 2008.
- [39] Ostriak A.V., Petrovsky V.P. Fire bench tests for strength of solid-fuel rocket engines to influence of lateral short-term loading. *Chemical physics*, Vol. 14, No. 1, pp.11-17, 1995.
- [40] Ostriak A.V. Settlement and experimental verification of strength of composite constructions of aircraft to mechanical action of x-ray radiation. *Questions of defensive techniques*, series 15, No. 1(168), pp. 8-17, 2013.

Copyright Statement

The authors confirm that they, and/or their company or organization, hold copyright on all of the original material included in this paper. The authors also confirm that they have obtained permission, from the copyright holder of any third party material included in this paper, to publish it as part of their paper. The authors confirm that they give permission, or have obtained permission from the copyright holder of this paper, for the publication and distribution of this paper as part of the ICAS 2014 proceedings or as individual off-prints from the proceedings.